INFLUENCE OF THE NON-LINEAR DYNAMIC RESPONSE OF SOILS IN THE PREDICTION OF SEISMIC RISK

Y.F. Vargas-Alzate[1], A.M. Zapata-Franco[2], J.R. Gonzalez-Drigo[3], L.G. Pujades[4] and J.V. Vaunat[5]

[1,2,4,5] Department of Civil and Environmental Engineering. Universitat Politècnica De Catalunya
Jordi Girona, 1-3, 08034, Barcelona, Spain
{ yeudy.felipe.vargas, ana.maria.zapata, lluis.pujades, jean.vaunat }@upc.edu

[3] Department of Structural Engineering. Universitat Politècnica De Catalunya
Jordi Girona, 1-3, 08034, Barcelona, Spain
jose.ramon.gonzalez@upc.edu

Abstract: *One of the key elements in characterizing the seismic response of civil structures is the local effect. It is because the expected ground motion acting on the foundation of a structure cannot be adequately described without considering the inelastic response of the soil near the surface. This response depends mainly on the parameters of the soil beneath the structure and the characteristics of the ground motion acting at depth, where nonlinear effects are negligible. Accordingly, enhanced mathematical arrangements to predict the nonlinear response of complex multi-degree-of-freedom systems can be developed if considering the dynamic properties of the soil and the main features of the ground motions acting at the bedrock. In this article has been analysed the probabilistic nonlinear response of steel buildings by considering the energy dissipation of the soil profile due to the pass of seismic waves. To do so, it has been used a recently proposed computational framework for assessing seismic risk, which is able to consider these interactions via Monte Carlo simulation. For this purpose, random soil profiles have been generated to obtain a representative sample of probable scenarios affecting the study area. Then, the ability of intensity measures (IM) to predict the dynamic response in the linear and nonlinear regimes of the structures have been assessed via Multi-regression analysis. Scalar-based and vector-valued IMs considering not only features of the ground motion at the bedrock level but also from the soil profile and the buildings have been analysed. Results have been processed by considering the number of stories of the buildings. It is observed that if the regression analysis is performed by considering the entire set of structures, the efficiency tends to decrease. Notwithstanding, there are some specific arrangements exhibiting high-efficiency in spite of the aggrupation.*

Keywords: Intensity Measures; Engineering Demand Parameters; Site effects; Multi-Regression Analysis

1 Introduction

Soil-structure interaction is becoming fundamental in the estimation of seismic risk (Cruz and Miranda, 2021). This is because the soil beneath the structure acts as the ultimate filter that amplify or de-amplify harmonics at specific frequencies. Accordingly, it is expected that structures with specific periods may enter into resonance with the soil. One of the most remarkable examples of this effect has been observed during the earthquake that affected Mexico City in 1985 (Beck and Hall, 1986). A significant amplification of long-period seismic waves was observed due to a very attenuated ground motion, as the earthquake occurred far from the city. This event shifted several conceptual paradigms of seismic risk estimation. Therefore, a key aspect of the seismic risk is the characterization of the dynamic response of the soil profile (Pagliaroli et al., 2014).

In line with the above, the frequency content of surface ground motions generated by earthquakes depends on several complex phenomena such as the type of rupture, location of the epicentre, depth and the mechanical properties of the media through which seismic waves pass. As observed in Mexico City, if the resulting ground motion at the surface has energy at frequencies similar to the fundamental one of a structure resting on this soil, the probability of resonance increases. This phenomenon highlights the need to study the soil-structure-interaction problem by considering both the probabilistic characteristics of the variables involved and their non-linear behaviour.

The use of advanced non-linear models considering soil-structure interaction has provided information to better understand this complex phenomenon (Pitilakis and Petridis, 2022). In this regard, it is common practice to use from simplified 1D soil models to advanced 3D finite-element-method-based representations (Fiorentino et al., 2019; Kaklamanos et al., 2015). However, the higher the complexity of the model, the longer the computational time required to solve dynamic problems. To address this computational effort, simplified soil models are widely used. One of the most employed is the 1D model, in which soil layers are considered as Kelvin-Voigt solids, (Hardin and Scott, 1967). This model is represented by a purely viscous damper and an elastic spring connected in parallel. In several cases, it provides a good approximation of the dynamic response of a soil profile. Furthermore, this model has been extended to consider nonlinearities associated with the loss of soil stiffness and the consequent increase in damping due to shear strains (Yoshida et al., 2002).

Regarding cutting-edge approaches for assessing seismic risk, the probabilistic characterization of the seismic hazard at a site is evolving from the hypothesis of ‘Uniform Hazard Spectrum’ (UHS) to the ‘Uniform Risk Spectrum’ one (URS). This latter allows ensuring that structures in different regions have the same collapse probability in the face of potential earthquakes. One of the main inputs to develop an URS is a collapse fragility function. This function should be representative of a large set of structural typologies. However, it may exhibit a large dispersion if it is derived with respect to an Intensity Measure (IM) with low steadfastness. This statistical property allows grouping results stemming from the dynamic response of several structural types without diminishing the efficiency to predict them. Therefore, using IMs with this property may lead to enhance the reliability related to predictions based on URS. In addition, the number of structural typologies to characterize urban settings for seismic risk assessment can be reduced.

This article has been focused in employing a recently developed computational framework for seismic risk assessment (Zapata-Franco et al., 2023) to analyse the steadfastness (Vargas-Alzate et al., 2022) of several IMs when predicting the nonlinear response of buildings. This computational framework is capable of simultaneously considering in a probabilistic manner: i) the main characteristics of ground motions acting at the bedrock level; ii) the dynamic soil properties and their evolution due to the degradation caused by the seismic waves; and iii) the main features influencing the dynamic behavior of buildings. Although this framework has been originally developed for Reinforced Concrete structures, due to its versatility, it has been easily adapted to analyse the response of steel structures. Therefore, the efficiency of a large set of Scalar-based and vector-valued IMs, which consider the main three elements allowed by the computational framework, has been analysed. Multi-regression analysis has been employed to do so. It has been observed that several IMs loss efficiency when grouping results stemming from buildings of different heights. However, there are some mathematical arrangements exhibiting high-efficiency in spite of this grouping. These advanced IMs can be employed to diminish uncertainties in seismic risk predictions.

Bogotá city has been selected as a study site since there are several soft soil deposits which may amplify seismic waves at long-periods. Moreover, there is a large database of soil profiles that facilitates the random characterization of the dynamic properties of the soil, (FOPAE, 2011). Three type of regressions have been compared: i) analysis of the bivariate distribution between Scalar-based IMs acting at the base of the soil profiles with parameters representing the nonlinear response of the building (e.g. The Maximum Inter-Storey Drift Ratio, MIDR, and the Maximum Floor Acceleration, MFA); ii) analysis of the bivariate distribution between Vector-valued IMs composed of two terms and the MIDR and MFA; iii) analogue to the latter but the Vector-valued IMs are composed of three terms. Results indicate that if the aggrupation is performed by considering buildings of low-rise (3-8 stories), mid-rise (9-14 stories) and high-rise (15-20 stories), the efficiency loss is much lower compared to the grouping of the total set of buildings used in this study, i.e. 3-20 storeys.

2 Probabilistic soil model

A probabilistic soil model is generally used in geotechnical applications to consider the spatial (Vanmarcke, 1977) and temporal (Carrière et al., 2018) variability of soil properties, and their effects on civil structures. These models rely on statistics and probability theory to simulate soil features such as strength and stiffness, which can vary with location and time. In this article, the probabilistic soil model presented in (Zapata-Franco et al., 2023) has been employed. Figure 1 shows a sketch of the computational framework employed in this research. The variables presented within the soil profile scheme (shear modulus, density, damping and layer thickness, G_i, ρ_i, ξ_i and h_i, respectively) determine the dynamic features of the model.

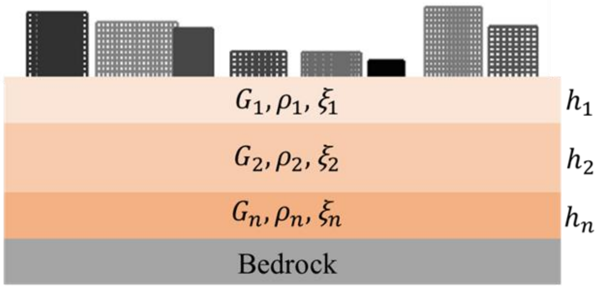

Figure 1. Schematic representation of the complete model

The probabilistic framework presented in (Zapata-Franco et al., 2023) allows for:

i. Introduce a ground motion record at the bedrock level of a soil profile.
ii. Estimate the stiffness degradation and increase of damping of each soil layer by using the equivalent linear method.
iii. Calculate the resulting ground motion at the surface after propagating seismic waves through the soil profile, taking into account the degradation of soil properties.
iv. The ground motion estimated in the previous step acts at the base of a probabilistic building model.

Accordingly, these steps have been applied after generating random samples of soil profiles and structures affected by ground motion records, which have been selected from a seismic database. These records have been acquired in seismic stations located in hard-soil.

2.1 Case of study: Bogotá Microzonation

Calculations have been made for a Lacustrine soil type, which is the most important deposit in Bogotá city. It is composed of soft clays with high compressibility, interspersed with lenses of loose sand, volcanic ash and peat that can reach a thickness of up to 1m. This soil type is characterized by sediment thicknesses ranging from 50m to 500m. In terms of dynamic properties, for lacustrine soil profiles with depths up to 200m, the fundamental period of vibration fluctuates between 1.1s and 2.6s, with shear wave velocities, Vs, between 140-280 m/s. For profiles with depths between 200m and 300m, the fundamental period varies from 3.5 to 3.8 sec, whose Vs are in the range 260-290 m/s. Finally, for soil profiles that reach more than 300 m, the expected fundamental periods vary from 4.9 up to 5.8 sec, with a Vs in the range 280-340 m/s.

2.2 Application of the Toro's model to a Lacustrine soil type

Toro et al. (Silva et al., 1996) proposed a probabilistic model for the variation of shear-wave velocity in soil and rock sites. It consists of three main elements: i) a model describing the random stratigraphy at the site; ii) the median Vs profile; and iii) a model describing the deviations of the Vs in each layer from the median, together with the correlation level with respect to the layer above. In sites where there is not enough information to directly characterizes uncertainties, this model appears to be an effective solution.

For soil parameterization, ten lacustrine profiles specified in the report (FOPAE, 2011) have been used. The random stratigraphy is characterized by using the "Layering Model" (Silva et al., 1996). This allows to consider that as the layer is deeper, it becomes thicker. In general, this model improves the prediction of ground motion intensity at the surface by providing a better picture of stratigraphic conditions at sites with different soil types. Hence, this model assumes that the thickness of each layer follows a depth-dependent probability distribution, where the thickness of layer *i* is independent of the thickness of layer *i*-1. The model also recognizes that soil layers tend to be thinner near the surface and thicker at greater depths (Silva et al., 1996). Accordingly, the following power law has been adopted to characterize the depth-dependent rate of layer boundaries:

$$\lambda(h) = C_3[h + C_1]^{-C_2} \tag{1}$$

where $\lambda(h)$ is the layer boundary rate (1/m) and *h* is the depth in m. The estimation of the terms C_1, C_2 and C_3 is carried out by using the capabilities of the Monte Carlo method to minimize multi-dimensional functions (Kucherenko et al., 2015). Therefore, to estimate the probable evolution of $\lambda(h)$, the entire number of layers composing the ten-initial set of soil profiles (193 layers) have been used.

Due to the cumulative process associated to the creation of sedimentary deposits, it has been observed that a log-normal distribution parametrizes adequately the aleatory character of Vs (Toro, 2022); this parametric distribution has been adopted in the sampling process. Note that, according to the Toro's model, the velocity is estimated at the layer midpoints. Another important aspect observed in soil profiles is related to the spatial correlation between closer layers. The closer the layers the higher the correlation of specific soil properties (Angelini and Heuvelink, 2018). In order to consider the likely correlation exhibited by the Vs between closer layers, it is necessary to employ a correlation hypothesis (Vargas Alzate et al., 2018). It has been assumed that the correlation between adjacent soil layers decreases with distance by means of the following model:

$$\rho_{i,j} = \begin{cases} i = j & \rho_{i,j} = 1 \\ i = j \pm k & \rho_{i,j} = 1 - \dfrac{k}{r} \geq 0 \end{cases} \tag{2}$$

where *k* is a number related to the position of a layer belonging to the same profile; *r* is a coefficient associated to the rate of correlation between adjacent layers. In this research, *r* has been fixed to 100/3.

Based on the statistical features described above, the Monte Carlo simulation has been employed to simulate one-thousand random soil profiles, as shown in (Zapata-Franco et al., 2023). These models have been used to analyse the efficiency and steadfastness of IMs.

3 Seismic hazard characterization

3.1 Selection and scaling of ground motion records

Accurate seismic hazard characterization is essential for a number of reasons, including risk assessment, effective planning and informed decision-making to prevent potential earthquake-related risks. In order to obtain a more precise representation of the seismogenic environment of Bogotá, an algorithm has been employed to identify the seismic records acquired in the stations closest to a study point within the Colombian territory (Zapata-Franco et al., 2023). It starts by taking an entire set of 1992 ground motions and collecting the relevant information such as: date of the seismic event, magnitude, station name, epicentral and hypocentral distance. Then, based on the coordinates of the studied area, and the maximum radius around this point, the nearest stations are identified and the signals recorded are extracted and addressed to two folders depending on whether the station is located on soil or rock. In parallel, a map that allows to identify the analysed point, and the stations delimited within the radius, is created. Moreover, the program provides the acceleration, velocity and displacement spectra. By using this program, it has been selected one-thousand ground motion records around Bogotá; a radius of 400 km has been used.

In spite of the large set of ground motion records identified, it is not common to find enough records exhibiting high intensity values in current seismic databases. This can derive to excessive scaling, which may introduce bias in the structural response (Haselton C.B., 2012). To address this issue, the method proposed by Vargas-Alzate et al., 2022b to select and scale ground motion records has been used. Figure 2 (Left) shows the spectra of the scaled records. The IM selected for scaling has been AvSa (Vargas-Alzate et al., 2022).

3.2 Seismic wave propagation by considering a 1D model

One dimensional site response analysis is associated with vertically propagating shear wave through horizontal layered media. To account for material damping, soil layer is modeled as a Kelvin-Voigt solid. This is a material whose resistance to shearing deformation is the summation of the elastic and viscous parts (Kumar and Mondal, 2017). Numerically, site response analysis based on 1D models can be performed using linear, equivalent linear and nonlinear methodologies. Amongst them, equivalent linear is widely followed because of its simplicity and reasonable accuracy with respect to non-linear-based results (Yoshida et al., 2002). This method consists of estimating, from iterative linear approximations, the physical properties of an analogous soil profile whose dynamic response is similar to that obtained by an exhaustive yet computationally expensive method, such as the non-linear dynamic analysis. These calculations are performed in the frequency domain, which substantially reduces the computational effort. This methodology has been used here to assess the stiffness degradation and the consequent increase in damping within the soil profile.

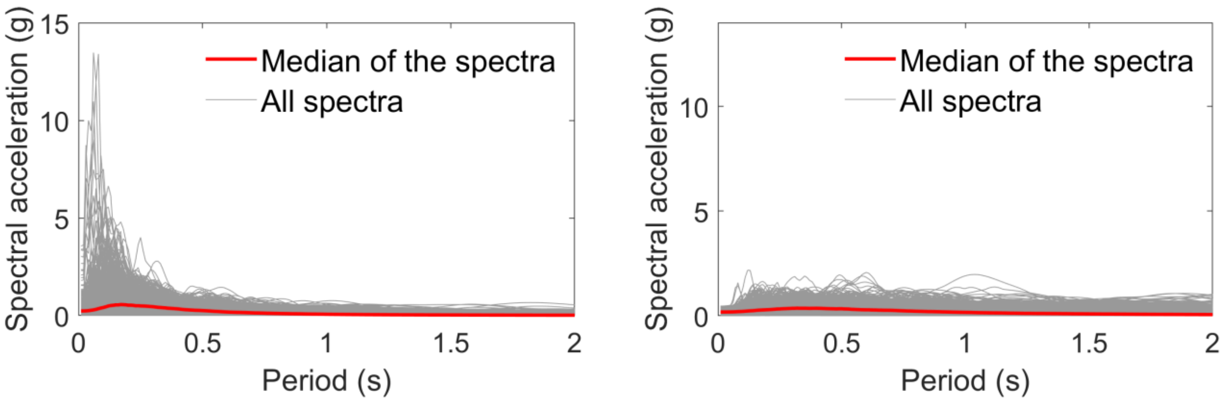

Figure 2 Left: Spectra of ground motion records acting at bedrock level. Right: Spectra of the resulting ground motions at the surface after the propagation process

In the equivalent linear method, the degradation of the stiffness, and the consequent increase in the damping, are considered by using the normalized shear modulus (G_0/G_{max}) and hysteretic damping curves; both as a function of the maximum shear strain reached during the dynamic process. For the case of study, the reference curves have been selected from the geotechnical report (FOPAE, 2011). Thus, by using both the scaled ground motion (see section 3.1) and the soil profiles described in section 2, the equivalent linear method has been employed to estimate the resulting ground motion at the surface. Figure 2, right, shows the resulting spectra at the surface level. These ground motion have been applied at the base of the steel structures, simulated in the next section, to perform nonlinear dynamic analyses, NLDA.

4 Generation of the probabilistic structural models

In terms of the structural characterization for large population of buildings, the acting loads and mechanical properties of the materials are the most important variables (Vamvatsikos and Fragiadakis, 2009; Vargas-Alzate et al., 2019). In addition, information regarding the geometrical distribution of buildings is also required (Silva et al., 2015; Vargas-Alzate et al., 2020). In the framework of the KaIROS project, a set of computer programs to generate structural models considering such uncertainties have been developed (Vargas-Alzate, 2018). This software has been employed in this article to perform part of the simulations. Specifically, a set of probabilistic numerical models representing the behaviour of Steel Moment resisting Frames (SMF), with beams and columns of Steel W type sections, have been simulated. Further details regarding the characterization of these structural models can be found in (Díaz et al., 2018).

4.1 Acting loads and mechanical properties of the materials

Mean values for live, *LL*, and permanent, *DL*, loads have been assumed Gaussian with the mean, μ, standard deviation, σ, and coefficient of variation (σ/μ) values shown in Table 1. Because of its large scattering, a higher coefficient of variation has been assigned to *LL* than to *DL*. However, only a fraction (30%) of the total design load has been considered for *LL*.

Due to the high-quality control related to the steel production, low variability is expected in the mechanical properties of this material. Anyhow, it has been preferred to take it into account within the probabilistic model. Accordingly, the tensile strength, *fy*, and the elastic modulus, *Es*, of the steel have been considered as random variables. Since these variables are highly correlated, a coefficient of correlation equal to 0.8 has been considered when sampling them; continuous Gaussian distributions have been assumed to represent these variables. μ, σ, and σ/μ values are also shown in Table 1.

Nonlinear behaviour is allowed at the end of beams and columns by considering a bilinear hysteresis rule. The strength and ductility parameters have been calculated according to the modified Ibarra-Medina-Krawinkler

Model (IMK, (Lignos et al., 2019; Lignos and Krawinkler, 2011)). Similar modelling approaches have been followed in (Díaz et al., 2018; Pinzón et al., 2020).

Table 1 Statistical parameters considering in the generation of the probabilistic models

	SMF frames		
	μ (kPa)	**σ (kPa)**	**σ/μ**
LL	1	0.1	0.10
DL	5	0.2	0.04
fy	4.2e5	2.1e4	0.05
Es	2.1e8	0.84e7	0.04

4.2 Geometrical properties

Modelling the random variation in building-to-building structural characteristics within a structural typology is standard practice (FEMA, 2018). In this respect, (Vargas-Alzate, 2018) developed a computer code to generate probabilistic multi-degree-of-freedom systems. Although they developed this program for reinforced concrete models, it has been easily adapted to generate structural steel ones (Pinzón et al., 2020). Accordingly, it has been generated one-thousand structural steel models whose number of stories, N_{st}, number of spans, N_{sp}, story height, H_{st}, and span length, S_l, have been considered random variables. N_{st} and N_{sp} are uniform discrete distributions within the intervals (3, 20) and (3, 6), respectively. H_{st} and S_l are uniformly distributed in the interval (3.3, 3.7) and (5, 7) m, respectively.

The structural elements presented in Table 2 have been adopted to assign the cross-sectional properties of the columns and beams of the first story, depending on N_{st}. For upper stories, the column and beam types reduce each 3 stories to the next section with lower properties according to Table 2. Figure 3 (Left) shows one-hundred of the generated models. The structural sections presented in Table 2, and the mechanical property values shown in Table 1, have been adjusted so that the generated models approximate the dynamic properties of SMF structures located in earthquake-prone areas. This can be verified by comparing the fundamental period of these models with the following approximation provided by (ASCE/SEI 7-16, 2017):

$$T_1 = 0.0724H^{0.8} \tag{3}$$

where T_1 represents the fundamental period and H the height of the building in meters. Figure 3 (Right) shows the evolution of T_1 as a function of H; T_1 values observed agree with those expected for the typology analysed.

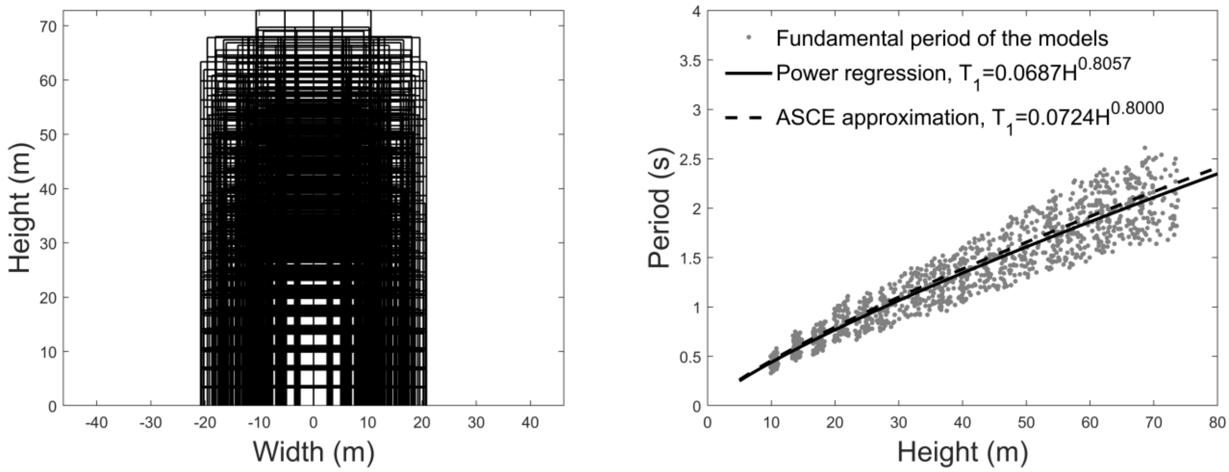

Figure 3 Left: One-hundred structural models. Right: Fundamental period vs height of the models

5 Intensity measures and engineering demand parameters

From a data set of ground motion records, basic mathematical background along with proper numerical tools allow extracting variables representing the seismicity of an area. In the context of earthquake engineering, such variables are known as IMs. Ideally, an IM should contain enough information about the earthquake, so according to it, the structural response can be predicted with confidence (Pejovic and Jankovic, 2015). Notice that an IM can depend either on the ground motion record, or on both the ground motion and structural features (Eads et al., 2015). In this article, information related to the soil properties arises to increase the efficiency of the IMs.

Table 2 Steel W sections assigned to the first-floor elements

N_{st}	***Column***	***Beam***	N_{st}	***Column***	***Beam***
3	W18x119	W14x68	**12**	W30x173	W18x97
4	W18x119	W14x74	**13**	W30X191	W18x106
5	W27x161	W14x74	**14**	W30X191	W18x106
6	W27x161	W14x74	**15**	W30X191	W18x106
7	W27x161	W16x89	**16**	W30X191	W18x119
8	W27x161	W16x89	**17**	W33X201	W18x119
9	W30x173	W16x89	**18**	W33X201	W18x119
10	W30x173	W18x97	**19**	W33X201	W21x132
11	W30x173	W18x97	**20**	W33X201	W21x132

5.1 Intensity measures

Spectral- and Energy-based IMs have been analysed in this research. They correspond to IMs derived from the dynamic equilibrium equation for single degree of freedom systems, SDoF. Particularly, the spectral-based IMs analysed in (Zapata-Franco et al., 2023) have been used in this research. In addition, it has been included four new IMs, which can be calculated as follows:

$$Sa_w = \sum_{i=1}^{3} Sa(T_i) * w_i \tag{4}$$

$$Sv_w = \sum_{i=1}^{3} Sv(T_i) * w_i \tag{5}$$

$$Sd_w = \sum_{i=1}^{3} Sd(T_i) * w_i \tag{6}$$

$$VE_w = \sum_{i=1}^{3} VE(T_i) * w_i \tag{7}$$

where Sa_w, Sv_w, Sd_w and VE_w are the weighted spectral acceleration, velocity, displacement, and equivalent velocity, respectively; T_i and w_i denote the period and the mass participation factor, respectively, related to the mode *i* of the building.

5.2 Engineering demand parameters

The MIDR is one of the most used EDP when analysing the seismic performance of buildings. Specifically, this variable is used to control the design or assessing the vulnerability of buildings. For a story *j*, the evolution of the inter-story drift is given by:

$$IDR_j(t) = \frac{\delta_j(t) - \delta_{j-1}(t)}{h_j} \tag{8}$$

where $\delta_j(t)$ is the time-history displacement at the floor *j* of the structure; h_j represents the height of the story *j*. The maximum inter-story drift ratio at the story *j*, $MIDR_j$, can be calculated as follows:

$$MIDR_j = max\big(abs(IDR_j(t))\big) \tag{9}$$

Finally, the maximum inter-story drift ratio in the building, MIDR, is given by:

$$\mathrm{MIDR} = max\big[MIDR_1, MIDR_2 \ldots MIDR_{N_{st}}\big] \tag{10}$$

The Maximum Floor Acceleration, MFA, is an EDP highly associated to damage in non-structural components. It can be calculated by analysing the time-history response of each floor in terms of acceleration.

$$MFA_j = max\big(abs(a_j(t))\big) \tag{11}$$

where $a_j(t)$ is the time-history acceleration at the floor *j* of the structure. Thus, in order to estimate non-structural damage, the *MFA* observed in the building is given by:

$$MFA = max\left[MFA_1, MFA_2 \ldots MFA_{N_f}\right] \tag{12}$$

where N_f is number of floors of the structure.

6 Statistical analysis of IM-EDP clouds

Once defined and characterized seismic hazard and exposure, one-thousand NLDAs have been performed. The Ruaumoko software has been used to perform structural analyses (Carr, 2007). Then, the MIDR and the MFA have been calculated for each simulation. The resulting cloud of IM-EDP points have been employed to analyse some statistical properties related to the data variability. Two type of polynomials has been used to calculate the coefficient of determination, R^2, based on the following statistical model:

$$\ln EDP = \alpha_0 + \sum_{i=1}^{N_{IV}} \sum_{j=1}^{n} \alpha_{j+(i-1)*n} (\ln IV_i)^j + \varepsilon \tag{13}$$

This model allows multi-linear (*n*=1) and -quadratic (*n*=2) regression in the log-log space. In this way, several sources of information can be considered simultaneously to better predict a specific EDP. Three regressions have been compared: i) analysis of the bivariate distribution between Scalar-based IMs acting at the base of the soil profiles with the MIDR and MFA; ii) analysis of the bivariate distribution between Vector-valued IMs composed of two terms and both EDPs (MIDR and MFA); iii) analogue to the latter but the Vector-valued IMs are composed of three terms. The objective is to analyse how much the efficiency increases when considering information related to the soil properties as well as to the buildings.

For the first regression case, the bivariate distribution between the entire set of IMs and both EDPs (MIDR and MFA) have been analysed. Figure 4 and Figure 5 show these clouds of points for MIDR and MFA, respectively. For MIDR, the most efficient IM is Sd_w whilst for MFA is Sv_w; both IMs contain information on the ground motion record and the building.

For regression cases 2 and 3, in addition to the entire set of IMs presented in Figure 4 and Figure 5, information regarding the soil properties have also been included to develop advanced vector-valued IMs; Table 3 presents the soil properties considered in this research.

Table 3 Soil properties considered in the development of vector-valued IMs

Variables	Equation	Description
T_{S_L}	$\sum_{i=1}^{nlayer} T_{S_{L,i}}$	Fundamental period of the soil profile
$\bar{\xi}_{NL}$	$\frac{\sum_{i=1}^{nlayer} \xi_{NL,i}}{nlayer}$	Average nonlinear damping of the soil profile
$\bar{\rho}_S$	$\frac{\sum_{i=1}^{nlayer} \rho_{S,i}}{nlayer}$	Average density of the soil profile
ΔT_s	$\lvert T_{S_{NL}} - T_{S_L} \rvert$	Absolute difference between the elongated and elastic period of the soil profile
β_L	$\frac{1}{\left\lvert 1 - \left({T_{S_L}}/{T_B} \right)^2 \right\rvert}$	Dynamic amplification factor considering the fundamental period of the soil profile
ΔT_{NL}	$\lvert T_{S_{NL}} - T_B \rvert$	Absolute difference between the nonlinear period, $T_{S_{NL}}$, of the soil profile and the fundamental period of the building, T_B

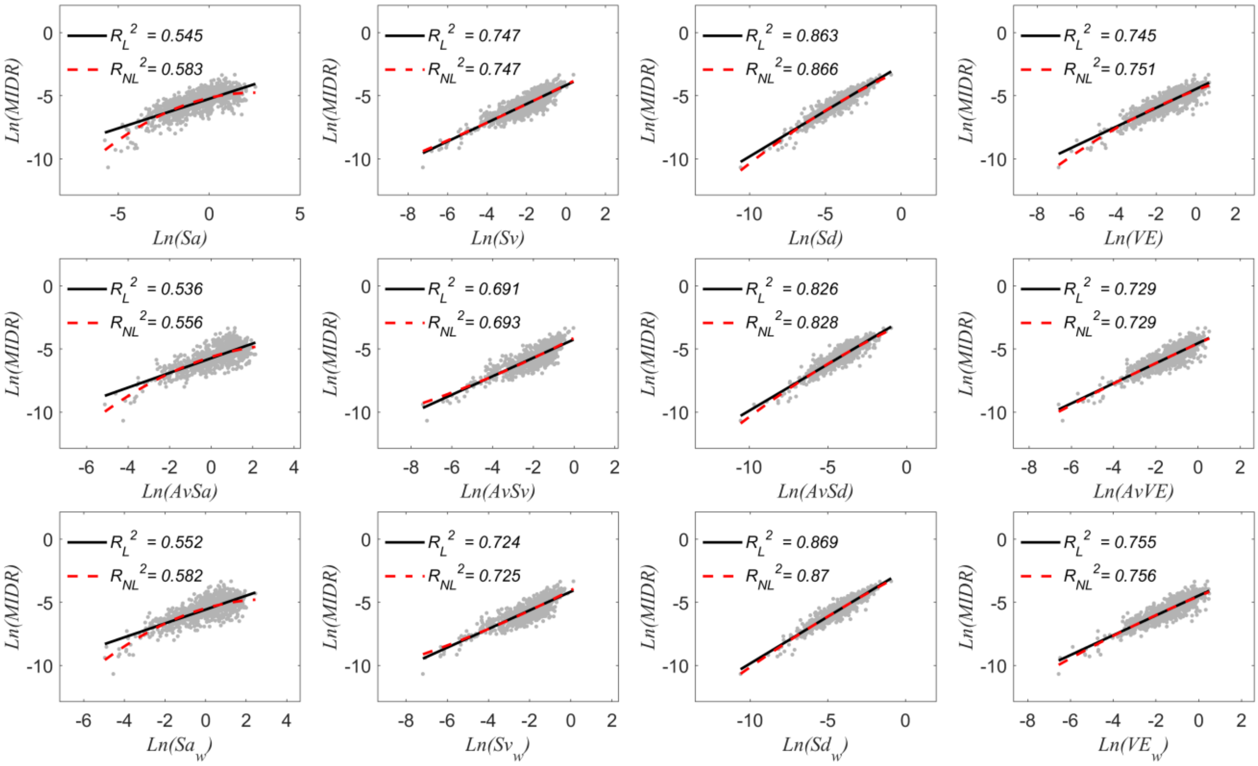

Figure 4 Bivariate distribution between spectral-based IMs and MIDR

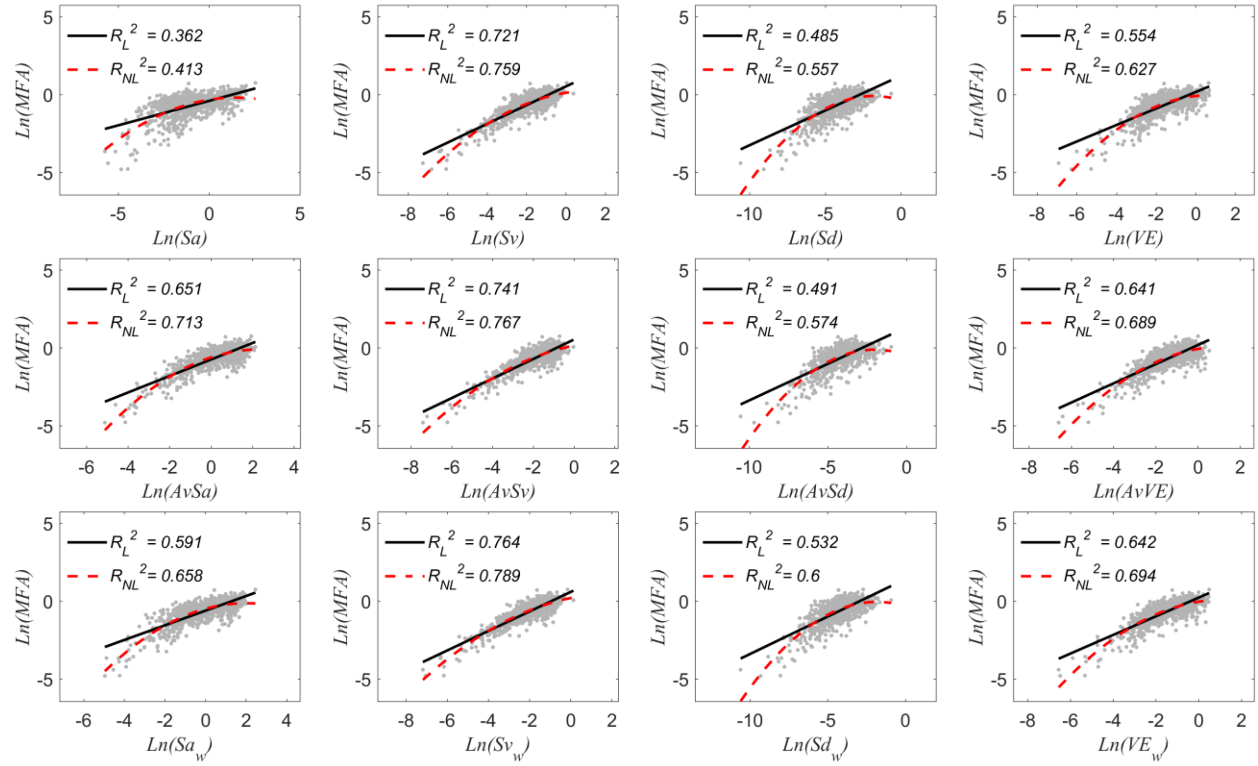

Figure 5 Bivariate distribution between spectral-based IMs and MFA

Note that the results presented in Figure 4 and Figure 5 consider the entire set of results. However, R^2 may increase if considering sub-groups of the analysed structures. In this research, low-rise (3-8 stories), mid-rise (9-14 stories) and high-rise (15-20 stories) have been employed to create the sub-groups. Table 4 and Table 5 summarize the results by considering these groups when considering MIDR and MFA as EDP, respectively.

Table 4 Coefficient of determination for the regressions analysed using the MIDR as EDP

MIDR	**Regression Type 1**		**Regression Type 2**			**Regression Type 3**			
Typology	$\boldsymbol{R^2}$	IM	$\boldsymbol{R^2}$	IM	$\mathbf{SV_1}$	$\boldsymbol{R^2}$	IM	$\mathbf{SV_1}$	$\mathbf{SV_2}$
Low	0.8741	Sd_w	0.9150	Sd_w	$\bar{\xi}_{NL}$	0.9227	Sd_w	T_{S_L}	$\bar{\xi}_{NL}$
Medium	0.8747	Sd_w	0.8914	Sd_w	ΔT	0.8990	Sd_w	ΔT	Sa_w
High	0.8990	Sd_w	0.9092	Sd_w	Sa	0.9180	Sd_w	$\bar{\rho}_S$	β_L
All	0.8700	Sd_w	0.8850	Sd_w	$\bar{\xi}_{NL}$	0.8937	Sd_w	$\bar{\xi}_{NL}$	$\bar{\rho}_S$

Table 5 Coefficient of determination for the regressions analysed using the MFA as EDP

MFA	**Regression Type 1**		**Regression Type 2**			**Regression Type 3**			
Typology	$\boldsymbol{R^2}$	IM	$\boldsymbol{R^2}$	IM	$\mathbf{SV_1}$	$\boldsymbol{R^2}$	IM	$\mathbf{SV_1}$	$\mathbf{SV_2}$
Low	0.8350	Sv_w	0.8879	Sv_w	$\bar{\xi}_{NL}$	0.9139	Sv_w	T_{S_L}	$\bar{\xi}_{NL}$
Medium	0.7133	Sv_w	0.8178	Sv_w	ΔT	0.8450	Sv_w	Sv	ΔT
High	0.7902	Sv_w	0.8396	Sv_w	ΔT	0.8751	Sv_w	Sv	ΔT
All	0.7886	Sv_w	0.8287	Sv_w	$\bar{\xi}_{NL}$	0.8658	Sv_w	ΔT_{NL}	$\bar{\xi}_{NL}$

7 Conclusions

In this article, the efficiency prediction of the non-linear dynamic response of steel frame structures has been analyzed. The aim has been to develop advanced IMs that consider the dynamic interaction between the building and the underlying soil. The non-linear behavior of the latter has been considered by employing the equivalent linear method (Yoshida et al., 2002). A set of probabilistic soil profiles, structural models, and ground motion records has been used in this research. They have been integrated within a probabilistic framework based on the Monte Carlo method, which allowed the identification of mathematical arrangement highly correlated to the EDP of interest. A 1D model to represent the soil profile has been employed to predict the intensity of ground motions at the surface, once the seismic waves generated by an earthquake reach the base of the building. In doing so, a large group of statistically compatible random soil profiles has been generated starting from the main features of a basic set of soil profiles. A database that collects almost two-thousand ground motion records acquired in Colombia has been used to characterize the seismic hazard.

The relationship between IMs and EDPs has been characterized using both linear and non-linear regressions in the log-log space. In this respect, the linear least squares model (See Eq (13)) allows for different types of regression, and it can be used to extract statistical information from IM-EDP pairs. It allowed to identify the most efficient IMs to predict the MIDR and MFA. This efficiency has been tested by considering the entire set of buildings as well as three sub-groups based on the number of stories.

First, the causal relationships between scalar-based IMs acting at the base of the soil profile and both EDPs have been analysed. From these results, it has been observed that, for MIDR, the most efficient IM is Sd_w, whilst for MFA is Sv_w. These advanced IMs contain information on the ground motion record and on the dynamic properties of the building. Particularly, these IMs consider the three most important periods of vibration of the structures analysed, as well as the mass participation factor of each of them. This increased ability to predict can be attributed to the fact that the structures analysed have a significant participation of higher modes. Regarding the analysis of sub-groups of structures, it has been observed that the efficiency tends to increase when compared to the one calculated for the entire set of buildings. Nevertheless, the increment in efficiency is not significantly high. Note also that when assessing the efficiency of sub-groups, for both EDPs, the governing IMs are the same as in the analysis considering all structures, i.e. Sd_w for MIDR and Sv_w for MFA. This indicates that these IMs are steadfast, according to the definition presented in (Vargas-Alzate et al., 2022).

The second approach has been to analyse the bivariate distribution between vector-valued IMs composed of two terms and both EDPs (MIDR and MFA). To do so, information regarding the soil profile properties have also been considered. In this case, it has been observed an increase in efficiency to predict both EDPs. Most importantly, in all of the cases studied, Sd_w for MIDR and Sv_w for MFA appear in the mathematical arrangements. It should also be noted that $\bar{\xi}_{NL}$ is the most efficiency-enhancing soil variable when the whole set of structures has been analysed. This variable also appears in some of the subgroups analysed. As for the third approach, similar conclusions can be drawn to those observed for the second case. It is worth mentioning that, when considering three variables for developing the vector-valued IMs (Third approach), the increased efficiency observed in MFA, when compared to the first and second approaches, is more significant.

Future research should be oriented to analyse the behaviour of MI considering other soil types, seismogenic environments and structural typologies. It should also be of interest to analyse the behaviour of new MI and more information variables in order to find more improved mathematical arrangements to predict the non-linear response of civil structures.

8 Acknowledgment and funding

This research has been funded by the Spanish Research Agency (AEI) of the Spanish Ministry of Science and Innovation (MICIN) through the projects with references: PID2020-117374RB-I00/AEI/10.13039/501100011033 and TED2021-132559B-I00 – J-02970.

9 References

Angelini, M.E., Heuvelink, G.B.M., 2018. Including spatial correlation in structural equation modelling of soil properties. Spat Stat 25, 35–51. https://doi.org/10.1016/j.spasta.2018.04.003

ASCE/SEI 7-16, 2017. Minimum design loads and associated criteria for buildings and other structures.

Beck, J.L., Hall, J.F., 1986. Factors contributing to the catastrophe in Mexico City during the earthquake of September 19, 1985. Geophys Res Lett 13, 593–596. https://doi.org/10.1029/GL013i006p00593

Carrière, S.R., Jongmans, D., Chambon, G., Bièvre, G., Lanson, B., Bertello, L., Berti, M., Jaboyedoff, M., Malet, J.-P., Chambers, J.E., 2018. Rheological properties of clayey soils originating from flow-like landslides. Landslides 15, 1615–1630. https://doi.org/10.1007/s10346-018-0972-6

Carr, J., 2007. Ruaumoko-Inelastic Dynamic Analysis Program.

Cruz, C., Miranda, E., 2021. Insights into damping ratios in buildings. Earthq Eng Struct Dyn 50, 916–934. https://doi.org/10.1002/eqe.3356

Díaz, S.A., Pujades, L.G., Barbat, A.H., Hidalgo-Leiva, D.A., Vargas-Alzate, Y.F., 2018. Capacity, damage and fragility models for steel buildings: a probabilistic approach. Bulletin of Earthquake Engineering 16, 1209–1243. https://doi.org/10.1007/s10518-017-0237-0

Eads, L., Miranda, E., Lignos, D.G., 2015. Average spectral acceleration as an intensity measure for collapse risk assessment. Earthq Eng Struct Dyn 44, 2057–2073. https://doi.org/10.1002/eqe.2575

FEMA, 2018. Seismic Performance Assessment of Buildings.

Fiorentino, G., Quaranta, G., Mylonakis, G., Lavorato, D., Pagliaroli, A., Carlucci, G., Sabetta, F., Della Monica, G., Lanzo, G., Aprile, V., Carlo Marano, G., Briseghella, B., Monti, G., Squeglia, N., Bartelletti, R., Nuti, C., 2019. Seismic Reassessment of the Leaning Tower of Pisa: Dynamic Monitoring, Site Response, and SSI. Earthquake Spectra 35, 703–736. https://doi.org/10.1193/021518EQS037M

FOPAE, 2011. Procesamiento e interpretación de señales de la red de acelerógrafos de Bogotá 2009 - 2011. Bogotá.

Haselton C.B., W.A.S., H.A., B.J.W., B.J. and G.D.N., 2012. Selecting and Scaling Earthquake Ground Motions for Performing Response-History Analyses . 15th World Conference on Earthquake Engineering, Lisboa, Portugal.

Kaklamanos, J., Baise, L.G., Thompson, E.M., Dorfmann, L., 2015. Comparison of 1D linear, equivalent-linear, and nonlinear site response models at six KiK-net validation sites. Soil Dynamics and Earthquake Engineering 69, 207–219. https://doi.org/10.1016/j.soildyn.2014.10.016

Kucherenko, S., Albrecht, D., Saltelli, A., 2015. Exploring multi-dimensional spaces: a Comparison of Latin Hypercube and Quasi Monte Carlo Sampling Techniques.

Kumar, A., Mondal, J.K., 2017. Newly Developed MATLAB Based Code for Equivalent Linear Site Response Analysis. Geotechnical and Geological Engineering 35, 2303–2325. https://doi.org/10.1007/s10706-017-0246-4

Lignos, D.G., Hartloper, A.R., Elkady, A., Deierlein, G.G., Hamburger, R., 2019. Proposed Updates to the ASCE 41 Nonlinear Modeling Parameters for Wide-Flange Steel Columns in Support of Performance-Based Seismic Engineering. Journal of Structural Engineering 145. https://doi.org/10.1061/(ASCE)ST.1943-541X.0002353

Lignos, D.G., Krawinkler, H., 2011. Deterioration Modeling of Steel Components in Support of Collapse Prediction of Steel Moment Frames under Earthquake Loading. Journal of Structural Engineering 137, 1291–1302. https://doi.org/10.1061/(ASCE)ST.1943-541X.0000376

Pagliaroli, A., Lanzo, G., Tommasi, P., Di Fiore, V., 2014. Dynamic characterization of soils and soft rocks of the Central Archeological Area of Rome. Bulletin of Earthquake Engineering 12, 1365–1381. https://doi.org/10.1007/s10518-013-9452-5

Pejovic, J., Jankovic, S., 2015. Selection of Ground Motion Intensity Measure for Reinforced Concrete Structure. Procedia Eng 117, 588–595. https://doi.org/10.1016/j.proeng.2015.08.219

Pinzón, L.A., Vargas-Alzate, Y.F., Pujades, L.G., Diaz, S.A., 2020. A drift-correlated ground motion intensity measure: Application to steel frame buildings. Soil Dynamics and Earthquake Engineering 132, 106096. https://doi.org/10.1016/j.soildyn.2020.106096

Pitilakis, D., Petridis, C., 2022. Fragility curves for existing reinforced concrete buildings, including soil–structure interaction and site amplification effects. Eng Struct 269, 114733. https://doi.org/10.1016/j.engstruct.2022.114733

Silva, V., Crowley, H., Varum, H., Pinho, R., Sousa, L., 2015. Investigation of the characteristics of Portuguese regular moment-frame RC buildings and development of a vulnerability model. Bulletin of Earthquake Engineering 13, 1455–1490. https://doi.org/10.1007/s10518-014-9669-y

Silva, W.J., Abrahamson, N., Toro, G., Constantino, C., 1996. Description and validation of the stochastic ground motion model. Pacific Engineering and Analysis.

Toro, G.R., 2022. Uncertainty in Shear-Wave Velocity Profiles. J Seismol 26, 713–730. https://doi.org/10.1007/s10950-022-10084-x

Vamvatsikos, D., Fragiadakis, M., 2009. Incremental dynamic analysis for estimating seismic performance sensitivity and uncertainty. Earthq Eng Struct Dyn n/a-n/a. https://doi.org/10.1002/eqe.935

Vanmarcke, E.H., 1977. Probabilistic Modeling of Soil Profiles. Journal of the Geotechnical Engineering Division 103, 1227–1246. https://doi.org/10.1061/AJGEB6.0000517

Vargas-Alzate, Y.F., 2018. KaIROS Project [WWW Document]. Polytechnic University of Catalonia. URL https://kairoseq.upc.edu/en

Vargas-Alzate, Y.F., Hurtado, J.E., Pujades, L.G., 2022. New insights into the relationship between seismic intensity measures and nonlinear structural response. Bulletin of Earthquake Engineering 20, 2329–2365. https://doi.org/10.1007/s10518-021-01283-x

Vargas Alzate, Y.F., Pujades Beneit, L.G., Barbat, A.H., Hurtado Gomez, J.E., Diaz Alvarado, S.A., Hidalgo Leiva, D.A., 2018. Probabilistic seismic damage assessment of reinforced concrete buildings considering directionality effects. Structure and Infrastructure Engineering 14, 817–829. https://doi.org/10.1080/15732479.2017.1385089

Vargas-Alzate, Y.F., Pujades, L.G., González-Drigo, J.R., Alva, R.E., Pinzón, L.A., 2019. On the equal displacement aproximation for mid-rise reinforced concrete buildings, in: Proceedings of the 7th International Conference on Computational Methods in Structural Dynamics and Earthquake Engineering (COMPDYN 2015). Institute of Structural Analysis and Antiseismic Research School of Civil Engineering National Technical University of Athens (NTUA) Greece, Athens, pp. 5490–5502. https://doi.org/10.7712/120119.7321.19849

Vargas-Alzate, Y., Lantada, N., González-Drigo, R., Pujades, L., 2020. Seismic Risk Assessment Using Stochastic Nonlinear Models. Sustainability 12, 1308. https://doi.org/10.3390/su12041308

Yoshida, N., Kobayashi, S., Suetomi, I., Miura, K., 2002. Equivalent linear method considering frequency dependent characteristics of stiffness and damping. Soil Dynamics and Earthquake Engineering 22, 205–222. https://doi.org/10.1016/S0267-7261(02)00011-8

Zapata-Franco, A.M., Vargas-Alzate, Y.F., Pujades, L.G., Gonzalez-Drigo, R., 2023. Improved intensity measures considering soil inelastic properties via multi-regression analysis. Front Earth Sci (Lausanne) 11. https://doi.org/10.3389/feart.2023.1214536